OPEN

Restoration of aquaporin-4 polarization in the spinal glymphatic system by metformin in rats with painful diabetic neuropathy

Chiliang Xu[a,*], Feixiang Wang[a,*], Can Su[b], Xiao Guo[a], Jiang Li[a] and Jingyan Lin[a,#]

Painful diabetic neuropathy (PDN) is a common complication in patients with diabetes, and its underlying mechanism remains unclear. Aquaporin-4 (AQP4) plays a crucial role in removing metabolic waste in the glymphatic system. In this study, we aimed to explore the relationship between the spinal glymphatic system and the effect of metformin on PDN. Male Sprague–Dawley rats were randomly allocated into the control group ($n = 10$), the PDN group ($n = 10$), and the metformin group ($n = 10$). A high-fat and high-glucose diet combined with low-dose streptozotocin was used to induce PDN rats. We detected the clearance rate of the contrast agent in the spinal cord of each rat by MRI to reflect the function of the glymphatic system. Immunofluorescence was used to detect the localization of perivascular AQP4 in astrocyte endfeet. Furthermore, we measured the expression of AQP4 in the spinal cord by Western blot. Compared with the rats in the control group, PDN rats exhibited enhanced mechanical allodynia, decreased clearance rate of the contrast agent in the spinal glymphatic system, reversed AQP4 polarization, and increased expression of AQP4. After being treated with metformin, the rats showed opposite changes in the above characteristics. The analgesic effect of metformin on PDN may be related to its ability to restore spinal AQP4 polarization, thus promoting the function of the spinal glymphatic system. *NeuroReport* **34: 190–197 Copyright © 2023 The Author(s). Published by Wolters Kluwer Health, Inc.**

NeuroReport 2023, **34**:190–197

Keywords: aquaporin-4, metformin, painful diabetic neuropathy, polarization, spinal glymphatic system

Departments of [a]Anesthesiology and [b]Radiology, the Affiliated Hospital of North Sichuan Medical College, Nanchong, China

[#]Correspondence to Jingyan Lin, PhD, Department of Anesthesiology, the Affiliated Hospital of North Sichuan Medical College, Nanchong, Sichuan, 637000, China
E-mail: linjingyan@nsmc.edu.cn; Tel: +86 8172598331

*Chiliang Xu and Feixiang Wang are cofirst authors.**Received** 24 October 2022 **Accepted** 9 January 2023.

Highlights

1. Aquaporin-4 (AQP4) played a crucial role in the clearance of metabolic waste in the spinal glymphatic system of painful diabetic neuropathy (PDN) rats. The polarization of perivascular AQP4 in the spinal cord is the key element of regulation.
2. The analgesic effect of metformin against PDN may be associated with its restoration of spinal AQP4 polarization, thus promoting the function of the spinal glymphatic system.

Introduction

Painful diabetic neuropathy (PDN) is the most common cause of neuropathy, and its morbidity increases with the duration of diabetes; it can negatively affect the sleep, mood, and functionality of the patient, leading to poor quality of life [1]. The pathogenesis of PDN is still unclear. Persistent activation of inflammation proteins in the peripheral nerves can induce central sensitization in PDN rats [2]. Scholars found that, in the central nervous system (CNS), an increasing number of synapses in the L5 spinal cord participated in the persistence of PDN [3]. Therefore, the CNS plays a crucial role in the pathogenesis of PDN.

Waste removal is essential to maintain the homeostasis and control function of the CNS. The CNS lacks unique lymphatic vessels to remove metabolic waste. The glymphatic system based on AQP4 water channels in astrocyte endfeet was recently found to be the excretion pathway for metabolic waste products of the CNS [4]. The glymphatic system is a brain-wide clearance pathway, and its impairment can cause the accumulation of β-amyloid protein, tau protein, and other waste, resulting in Alzheimer's disease and cognitive deficiency associated with diabetes [5–7]. Astrocytes are widely distributed on the surfaces of the brain and spinal cord. The pathway of the spinal glymphatic system has been confirmed in several studies [8,9]. Aquaporin-4 (AQP4) is a crucial aquaporin expressed in the CNS. The influx of CSF depends on the expression and perivascular localization of the AQP4. Abnormal expression and localization of AQP4 can lead to various CNS disorders, including

Supplemental Digital Content is available for this article. Direct URL citations appear in the printed text and are provided in the HTML and PDF versions of this article on the journal's website, www.neuroreport.com.

diabetes-related neuronal degeneration, impaired cognitive function, and Alzheimer's disease [10,11]. Metformin is a drug widely used to treat type 2 diabetes. This drug has been used for 60 years as a highly effective antihyperglycemic agent. Its possible mechanism is the effect on gluconeogenesis, protein metabolism, fatty acid oxidation, oxidative stress, glucose uptake, autophagy, and pain. Metformin has therapeutic effects on inflammatory pain, diabetic neuropathy pain, postchemotherapy pain, and postoperative pain [12]. Therefore, we designed a metformin group to observe the function changes in the spinal glymphatic system after metformin treatment.

Materials and methods

Animals

All experimental procedures were approved by the ethical committee of North Sichuan Medical College (No. 202183). The Guide for the Care and Use of Laboratory Animals (NIH Publications No. 8023, revised 1978) proposed by the National Institutes of Health guide was followed throughout the experiment. Fifty male adult Sprague–Dawley (SD) rats (bodyweight, 160–180 g; age, 6 weeks), specific pathogen-free grade, were obtained from the experimental animal center of North Sichuan Medical College. We used the method described by Lin *et al.* [13] to establish the animal model of PDN. All experimental rats were taken appropriate measures to reduce discomfort. All rats were fed in a single cage under a 12 h: 12 h light: dark cycle at 21–23 °C with no restriction on food and water. Ten rats were randomly selected and allocated to the control group and were maintained on a normal diet (57% carbohydrate, 22% protein, 6% fat, 8% cellulose, and 7% other elements). The other forty rats were maintained on a high-fat and high-glucose diet (60% control fodder, 20% sucrose, 15% lard, and 5% cholesterol). After feeding for 5 weeks, the rats were intraperitoneally injected with 1% streptozotocin (STZ, 25 mg/kg, sigma chemical, USA), whereas rats in the control group were intraperitoneally injected with an equal volume of sterile saline. Rats with fasting blood glucose (FBG) above 16.7 mmol/l were considered to have diabetes mellitus. The paw withdrawal threshold (PWT) was measured every 7 days after the increase of glucose, and the PDN model was considered successful after the PWT decreased significantly.

Metformin treatment

After 5 weeks of STZ injection, a total of 20 rats were successfully modeled and randomly divided into the PDN group (n = 10) and the metformin group (n = 10). Rats in the metformin group were treated by intragastric administration of metformin (hydrochloride metformin, Solarbio, Beijing, China, 200 mg/kg, dilute to 8% with ultrapure water) once a day for 4 weeks. Meanwhile, rats in the other two groups were treated by intragastric administration of an equal volume of ultrapure water. Furthermore, all animals were fed the same diet as before in this experiment. The blood glucose, PWT, and body weight were measured and recorded weekly.

Behavioral test

For the PWT measurement, the pain threshold on the soles of both feet of rats was evaluated using the 'up-down' method [13]. Animals were placed in transparent glass on a metal grid floor and acclimatized for 15 min before testing. When rats woke up without walking and licking their feet, von Frey filaments (NC12775-99, North Coast, California, USA, 0.06, 1, 2, 4, 6, 8, 10, 15, and 26 g) were applied perpendicularly to the bottom of the fourth and fifth toes of the hind feet. Starting with 0.06 g, each pressure stimulation was performed for 5 s with a 15-s interval between two stimulates. If there was no positive reaction, then the intensity of cilia increased. If there was a positive reaction, then stimulation continued five times. The positive reaction was defined as sudden shrink or foot licking. Otherwise, it would be recorded as a negative reaction. The PWT value was recorded for the force that could induce withdrawal responses three times in six stimulations. To avoid damage to the sole of rats, the maximum value of von Frey filament should not exceed 15 g. If 15 g cilia stimulation remained negative, 26 g was recorded as the PWT value.

Magnetic resonance imaging

The SD rats fasted for 12 h, drank water, and were in the prone position. Spontaneous breathing was maintained under sevoflurane inhalation anesthesia, with sevoflurane 2 l/min + oxygen 2 l/min inhalations. The body temperature was kept at 36.5–37.5 °C during imaging. All imaging protocols were performed on a 3.0 T MRI instrument (750Discover, General Electric Company, GE) and the animal special coil (eight-channel rat coil for GE). After scanning the basic value of the rat spinal cord, 25 μl 7.5% Magnevist (Gd-DTPA, Gadolinium-diethylenetriamine Penta-acetic acid, 469. 01 mg/ml, MW 938 Da, Bayer, Leverkusen, Germany) was slowly injected into the subarachnoid space of rats at L4–5 spaces in 5 min. After the injection, the puncture needle stayed in position for 3 min. Then, the scan was performed immediately. Scanning was performed before intrathecal injection of Gd-DTPA and 15, 30, 60, 90, 120, 150, 180, and 300 min after Gd-DTPA injection. During the absence of a scan, the rats were allowed to wake up, drank water freely, and were kept warm. The signal value was measured by the RadiAnt DICOM software (64bit, Version 2021.1, Medixant, Poznan, Poland). The spinal clearance rate equals the spinal cord signal difference (peak value minus 6th-hour signal intensity) divided by time.

Western blot

The protein samples (30 μg) were subjected to electrophoresis on a 10% Tris-HCl SDS-PAGE gel (Bio-Rad, Guangzhou, China) and transferred onto a PVDF membrane (PVDF, polyvinylidene fluoride; Immobilon-PSQ, Shanghai, China). After blocking nonspecific binding sites with 5% nonfat milk in 0.1% Tween-20/Tris-buffered saline (TBS-T) for 2 h at room temperature, membranes were incubated with primary antibody AQP4 (1:2500 Novus, NBP1-87679, USA) and β-actin (1:2000, Santa Cruz, sc-47778) for 12 h at 4 °C refrigerator. Then, membranes were washed with TBS-T and probed with a secondary antibody (goat anti-rabbit 1:5000 and goat anti-mouse 1:5000, Abcam, Cambridge, UK) for 2 h at room temperature. After washing, the protein bands were visualized using an enhanced chemiluminescence assay, according to the manufacturer's instructions. The signal intensity of the bound primary antibody was quantitatively analyzed with an imageJ analyzer and relative quantification of β-actin.

Immunofluorescence

The rest of the five rats in each group were selected for immunofluorescence. Rats were deeply anesthetized with 50 mg/kg of 10% chloral hydrate intraperitoneally and immobilized by transcardiac perfusion with 200 ml of sterile control saline and 200 ml of 4% paraformaldehyde in 0.1 mol/l PBS (PH, 7.4). After standard fixation, dehydration, transparency, and embedding, 4-μm paraffin sections were prepared. Three sections were sampled from 15 serial sections according to a systematic (equal spaced) manner. After dewaxing, hydration, and antigen repair, the sections were sealed with 5% goat serum for 60 min, and then, antigen staining was carried out. Primary antibody AQP4 (1:150, NBP1-87679, Novus) and CD31 (1:50, sc-376764, Santa Cruz) were incubated overnight at 4 °C, reheated at 37 °C for 30 min, and washed with PBS three times for 15 min each time. Vascular endothelial cells were labeled with CD31. Then, the secondary antibodies conjugated Alexa Fluor 647 (Abcam), AlexaFluor 488 (Abcam) secondary goat anti-rabbit IgG H&L antibodies (1:500, Abcam, ab150079), and goat anti-mouse IgG H&L antibodies (1:500, Abcam, ab150113) were sealed with anti-fluorescence quenching sealing solution with DAPI (DAPI, 4',6-diamidino-2-phenylindole Beyotime, p0131, Shanghai, China). The sections were observed under a laser confocal microscope (Olympus fv1200, Olympus, Tokyo, Japan). Fluorescence quantification was analyzed by the ImageJ software.

Quantification of aquaporin-4 polarization

To measure the perivascular AQP4 polarization, the method described by Harrison *et al.* [11] was used. Three sections/animal in each group were randomly selected and analyzed in a blinded manner using the ImageJ version 1.53e bundled with the Java 1.8.0_172 software (National Institutes of Health, Bethesda, Maryland, USA) by investigators blinded to treatment conditions. The ventral horn, dorsal horn, and central canal of each selected section were measured. To avoid the influence of nonspecific motor neuron staining on the measurements, we selected intact perivascular areas labeled with CD31. First, we split the channels of the images. Then, we selected the channel of the AQP4 image, used the system to automatically assign thresholds, and measured the median immunofluorescence intensity of perivascular areas. Finally, the proportion of AQP4 fluorescence intensity below the median immunofluorescence intensity of perivascular areas in the whole image was measured by threshold analysis. This proportion was expressed as AQP4 polarization.

Statistical analysis

We performed the statistical analysis using the GraphPad Prism software (GraphPad Prism 9.1.0, GraphPad, Beijing, China). These data were all expressed as means ± SEM and analyzed by one-way analysis of variance (ANOVA) or two-way ANOVA for repeated measurements followed by Tukey's multiple comparisons test. Probability values less than 0.05 are considered statistically significant.

Results

Brief flowchart of the experimental design

In our study, 50 rats were fed for 14 weeks. A total of 10 rats in the control group were fed with a normal diet, and 40 rats were fed with a high-fat and high-glucose diet. After 5 weeks of feeding, the rats fed with a high-fat and high-glucose diet were intraperitoneally injected with STZ, and rats in the control group were intraperitoneally injected with sterile saline. In the 10th week of feeding, 20 rats were considered successfully modeled as PDN rats and then randomly allocated into the PDN group ($n = 10$) and the metformin group ($n = 10$). The rats in the metformin group were treated with metformin, whereas the rats in the PDN group and control group were treated with equal ultrapure water for 4 weeks. In the 14th week of feeding, all rats were sequentially subjected to MRI, Western blot, and immunofluorescence experiments (Fig. 1).

Metformin attenuated the mechanical allodynia in diabetic rats

The body weight of the rats injected with STZ was lower than that in the control group (Fig. 2a; $P < 0.01$). The FBG of the rats increased significantly after intraperitoneal injection of STZ (FBG > 16.7 mmol/l), whereas that of PDN rats decreased significantly after treatment with metformin (Fig. 2b; $P < 0.01$). In addition, the rats injected with STZ showed polydipsia, polyphagia, polyuria, and a poor activity state. Based on these characteristics, we found that STZ successfully induced diabetic

Fig. 1

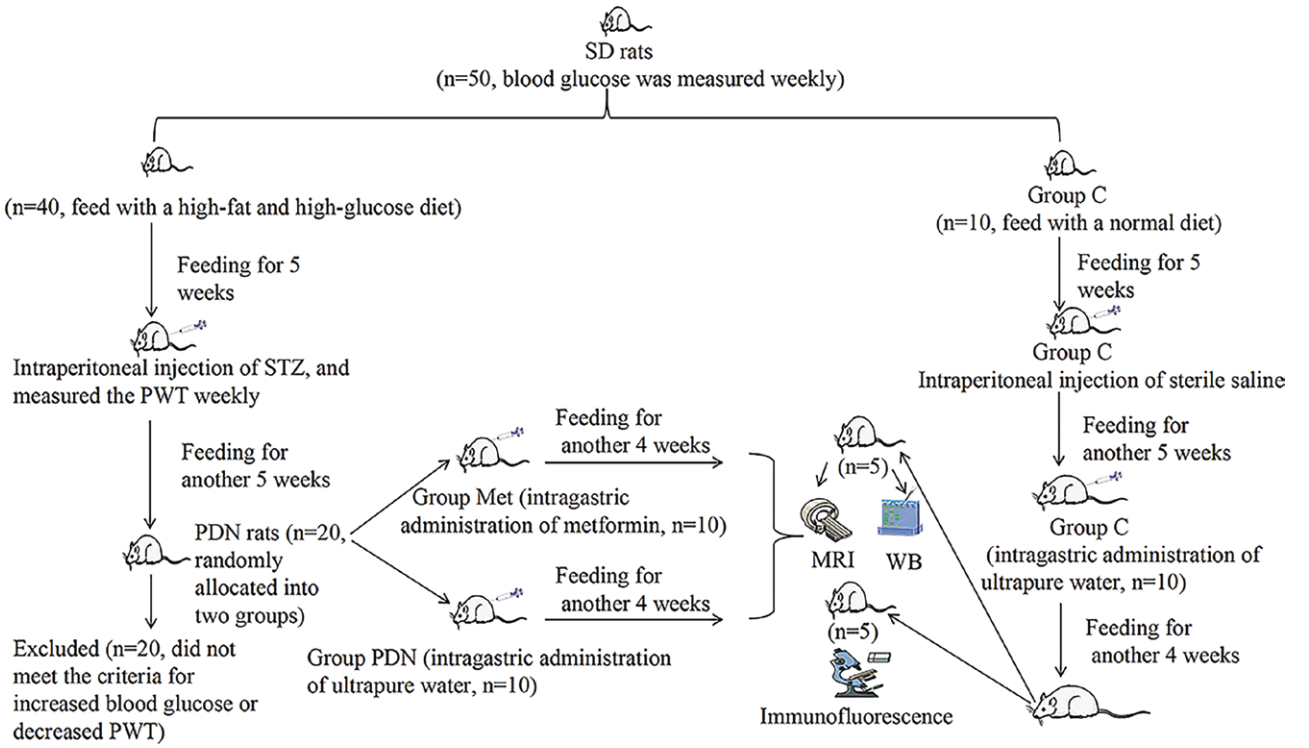

The brief flow chart of the experimental design. After 5 weeks of feeding, The PDN group rats were intraperitoneally injected with STZ, and the rats in the control group were intraperitoneally injected with sterile saline. Then, all the rats were observed for 5 weeks. After the pain threshold was stabilized, the rats in the metformin group were treated with metformin for 4 weeks. The MRI of the lumbar enlargement of the spinal cord was performed. The tissue of lumbar enlargement of the spinal cord was taken for Western blot and immunofluorescence. PDN, painful diabetic neuropathy; STZ, streptozotocin.

Fig. 2

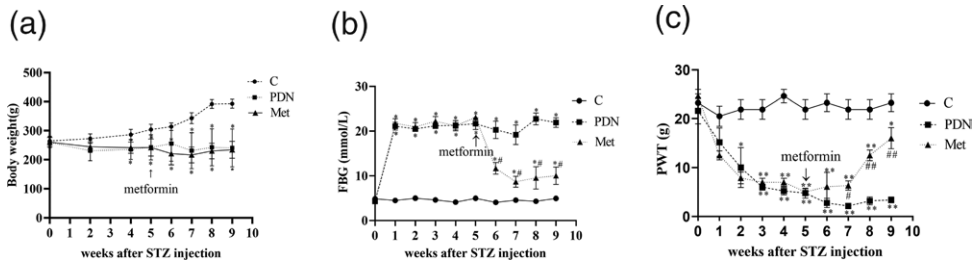

The trends of body weight, blood glucose, and PWT in the three groups. (a) The change in body weight after STZ injection. (b) The change in blood glucose after STZ injection. (c) The change in PWT after STZ injection. Data are presented as mean ± SEM ($n = 10$/group). Compared with the control group, $^{*}P < 0.05$, $^{**}P < 0.01$. Compared with the PDN group, $^{\#}P < 0.05$, $^{\#\#}P < 0.01$. FBG, fasting blood glucose; PDN, painful diabetic neuropathy; PWT, paw withdrawal threshold; STZ, streptozotocin.

rats. After 2 weeks of STZ injection, the PWT of the rats began to decrease. In the second week after the STZ injection, the rats showed obvious mechanical hyperalgesia. After 2 weeks of treatment, the pain threshold of the rats in the metformin group began to increase. In the fourth week after treatment with metformin, the pain threshold of the rats in the metformin group increased significantly compared with those in the PDN group. The result shows that metformin can effectively alleviate mechanical hyperalgesia in PDN rats (Fig. 2c; $P < 0.01$).

MRI showed the dynamic changes in Gd-DTPA in the glymphatic system of the rat spinal cord

The MRI signal intensity of lumbar enlargement of the spinal cord in each group changed dynamically with time after the subarachnoid injection of Gd-DTPA. The

glymphatic system can clear metabolic waste. As a tracer of metabolic waste, Gd-DTPA was tracked in the glymphatic system. Fifteen minutes after the injection of Gd-DTPA, the contrast agent was discontinuously distributed in the superficial pia mater of the spinal cord. Over time, a large amount of contrast agent entered the anterior and posterior horns of the spinal cord along the anterolateral sulcus, and the gray matter of the spinal cord showed a 'four-corner sign'. When the signal intensity of the contrast agent reached the peak value in lumbar enlargement, the gray matter of the spinal cord showed the brightest 'butterfly sign' and then gradually darkened. We selected the best images in the three upper and lower sections of the L5 segment of the rat spinal cord, so there were both large and small spinal cord images (Fig. 3a). The rats in the PDN group manifested a lower clearance rate of metabolic waste of the spinal cord than those in the control group. The clearance rate of metabolic waste was significantly higher in rats treated with metformin for 4 weeks than in those in the PDN group (Fig. 3b; $P < 0.01$).

Effects of metformin on the expression of aquaporin-4 in the spinal cord of diabetic rats

AQP4 is an important aquaporin. Compared with the expression of AQP4 in the rats in the control group, that in the PDN rats increased. After 4 weeks of metformin treatment, the rats showed decreased expression of AQP4 in the spinal cord (Fig. 4a and b; $P < 0.01$).

Quantitative analysis of the perivascular aquaporin-4 polarization

In this study, we used a new fluorescence quantitative research method [11]. The median immunofluorescence intensity of AQP4 in the perivascular areas was measured for the threshold analysis conducted by the ImageJ software. As shown in Fig. 5a and b and Table 1, compared with the AQP4 polarization in the perivascular areas of the rats in the control group, that of the PDN rats was reversed. In the zoomed-in image, the changes in perivascular AQP4 were visible to the naked eye. The AQP4 polarization of the rats in the control group was 64.87% (±2.58%), whereas that of the rats in the PDN

Fig. 3

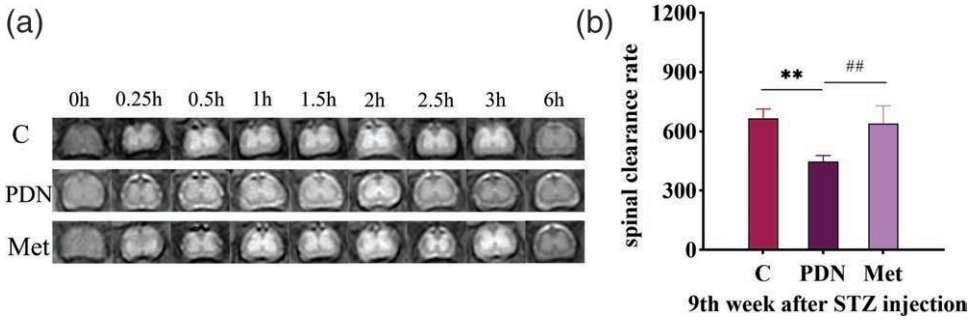

MRI showed the change in the signal intensity with time at the lumbar enlargement of the spinal cord in rats. (a) Gd-DTPA was injected into the subarachnoid space of the spinal cord at nine time points (0 min, 15 min, 30 min, 1 h, 1.5 h, 2 h, 2.5 h, 3 h, and 6 h). The signal intensity changed from dark to bright and then from bright to dark. The gray matter of the spinal cord showed an obvious 'butterfly sign'. No contrast agent signal existed in the white matter of the spinal cord of the rats in each group. (b) The spinal clearance rate = (peak value − 6th value)/interval. Data are presented as mean ± SEM ($n = 5$/group). In the ninth week after STZ injection, compared with the control group, $^{**}P < 0.01$; compared with the PDN group, $^{\#\#}P < 0.01$. PDN, painful diabetic neuropathy; STZ, streptozotocin.

Fig. 4

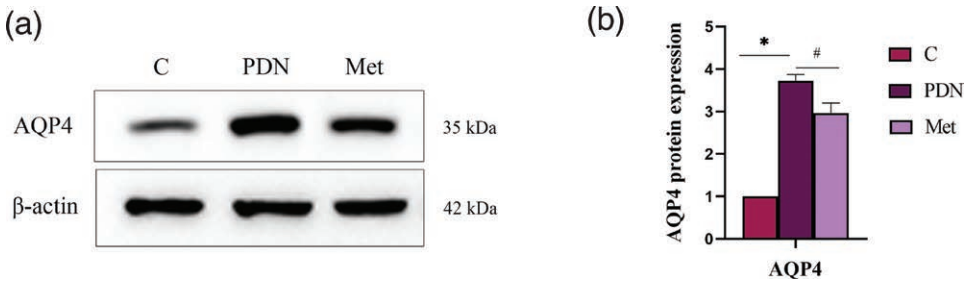

Western blot results. The tissue of the L5 segment of the rat spinal cord. (a and b) The levels of AQP4 were controlled to the relative intensity of β-actin ($n = 5$/group). Values were presented as mean ± SEM. Compared with the control group, $^{*}P < 0.05$. Compared with the PDN group, $^{\#}P < 0.05$. AQP4, aquaporin-4; PDN, painful diabetic neuropathy.

Fig. 5

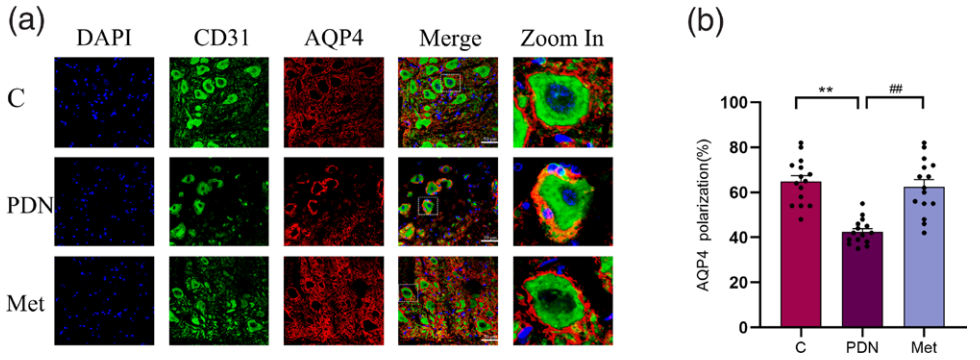

Immunofluorescence results. (a) The localization of perivascular AQP4 in the three groups. Immunofluorescence staining of sections using anti-CD31 and anti-AQP4 antibodies was obtained from the spinal cord L5 segment of each rat, including the ventral horn, dorsal horn and central canal on each selected section. Aquaporin-4 positive cells were identified with red fluorescence. Vascular endothelial cells were labeled with CD31. The CD31 positive cells were identified with green fluorescence, and the nuclei were counterstained with DAPI (blue). A typical part of reversed AQP4 polarization was zoomed in and shown in detail. Scale bar = 50 μm. (b) Data are presented as mean ± SEM ($n = 15$ sections/group). Compared with the control group, $^{**}P < 0.01$. Compared with the PDN group, $^{\#\#}P < 0.01$. AQP4, aquaporin-4; PDN, painful diabetic neuropathy.

Table 1 The MRI signal intensity, immunofluorescence quantification and Western blot results

Projects	Group C ($n = 5$)	Group PDN ($n = 5$)	Group Met ($n = 5$)	*P*-value
Preinjection SIa	6675 ± 449.9	7904 ± 757.4	8501 ± 339.5	0.09
Peak SIb	12 514 ± 963.4	13 164 ± 954.3	15 041 ± 1118	0.22
Six-hour SIc	9556 ± 1202	11 338 ± 854.2	12 796 ± 979.9	0.12
SIPHd	666 ± 21.35	446.4 ± 13.91**	639 ± 40.19$^{\#\#}$	<0.01
Peak SI timee	1.9 ± 0.36	2 ± 0.27	1.9 ± 0.29	0.39
AQP4 polarization (%)	64.87 ± 2.58	42.47 ± 1.44**	61.80 ± 1.66$^{\#\#}$	<0.01
Relative AQP4	1 ± 0	3.72 ± 0.15*	2.96 ± 0.23$^{\#}$	<0.01

Compared with the control group, $^{**}P < 0.01$. Compared with the PDN group, $^{\#\#}P < 0.01$. Compared with the control group, $^{*}P < 0.05$, $^{**}P < 0.01$. Compared with the PDN group, $^{\#}P < 0.05$, $^{\#\#}P < 0.01$.

AQP4, aquaporin-4; PDN, painful diabetic neuropathy; Met, Metformin; SI, signal intensity; SIPH, the peak hour of signal intensity.

[a]The preinjection signal intensity.

[b]The peak of signal intensity.

[c]The signal intensity six hours after the Gd-DTPA injection.

[d]The variation of the signal intensity per hour after it reached its peak (spinal clearance rate).

[e]The time to reach peak signal intensity (hour).

group was 42.47% (±1.44%) ($P < 0.01$), indicating the reversed AQP4 polarization of the rats in the PDN group. After 4 weeks of metformin treatment, the AQP4 polarization of the rats in the metformin group was 61.80% (±1.66%), whereas that of the rats in the PDN group was 42.47% (±1.44%) ($P < 0.01$). The above results indicate the reversed AQP4 polarization of the rats in the PDN group and the restored AQP4 polarization of the rats in the metformin group.

Discussion

This study revealed a neuroprotective mechanism by which metformin attenuates PDN by restoring the AQP4 polarization in the spinal glymphatic system. Due to the influence of estrogen, the blood glucose of female rats is unstable and may recover after STZ injection. Therefore, male SD rats were selected as the subjects in this study. Many diseases, such as Alzheimer's disease and cognitive deficiency related to diabetes, are associated with the impaired glymphatic system [5,6,14]. MRI is widely used to study the function of the glymphatic system [15]. Many substances, including metabolic waste, are in CSF. The GD-DTPA contrast agent used in this study was regarded as metabolic waste, and its clearance process and clearance rate in CSF were observed. After Gd-DTPA was injected into the L4–5 subarachnoid space, the MRI signal intensity of lumbar enlargement in each group changed dynamically with time. The contrast agent entered the anterior and posterior horns of the spinal cord along the anterolateral sulcus over time, showing a 'four-corner sign'. When the contrast agent reached its peak at the lumbar enlargement, the gray matter showed the brightest 'butterfly sign'. The peak time was usually about 2 h after injecting the contrast agent (Table 1). The gray matter of the spinal cord was bright, but the white matter was not. The possible reason is that the gray matter of the spinal cord is rich in arteriovenous vessels, whereas the white matter of the spinal cord consists mainly of fiber bundles, making it difficult for the contrast agent to enter. In this study, the signal intensity of preinjection, peak signal intensity, sixth-hour signal intensity, and peak time in each group were not statistically different between groups. However, the values in the PDN and metformin groups were higher than those in the control group, which may be related to inflammation in the spinal cord of PDN rats (Table 1). The clearance rate of the Gd-DTPA contrast agent in the spinal glymphatic system of living PDN rats was decreased, indicating impaired activity of the spinal glymphatic system in PDN rats. In addition, the clearance rate of the contrast agent was enhanced in living PDN rats after metformin treatment, demonstrating

that metformin enhanced the clearance rate of the contrast agent in the spinal glymphatic system of PDN rats. The vascular space of rats in the PDN group was larger and more dispersed (Fig. 5a). The enlargement of perivascular space is associated with diabetes, and the enlarged perivascular space may be one factor in reducing the clearance rate of Gd-DTPA [6]. The aggregation of inflammatory substances and glycation end products may also increase the perivascular space, leading to stagnant glymphatic transport, thus decreasing the clearance rate of the contrast agent in the spinal cord of living PDN rats [5,16]. The activity and efficiency of the spinal glymphatic system of PDN rats were impaired, and metformin could restore the impairment.

Astrocytes are an important structural foundation of the glymphatic system [17]. AQP4 belongs to a channel family that is selectively permeable to water. It is the most abundant water channel in the brain, spinal cord, and optic nerve and controls the water homeostasis in the brain [18]. AQP4 is highly selectively expressed in the blood–brain barrier and blood–CSF barrier and plays an important role in solute exchange and waste removal in the brain. The animal model with spinal cord injury has indicated that the increased abundance of AQP4 on the cell surface is related to cell swelling and essential for spinal cord edema [19,20]. The loss of AQP4 polarization means that the expression of AQP4 is mislocated and widely distributed in astrocytes rather than being focused on the endfeet surrounding blood vessels. The previous study has shown that an increase in AQP4 membrane localization in primary human astrocytes is not accompanied by changes in AQP4 expression levels [21]. The expression of AQP4 was higher in the PDN group than in the control group, but the polarization of perivascular AQP4 in PDN rats was reversed. We concluded that the normal distribution of AQP4 is more important than the expression level for water homeostasis. In order to avoid the interference of nonspecific staining for the quantification of AQP4 polarization, we selected blood vessels with complete structures and clear images to measure the median immunofluorescence intensity and delineated the red areas around the blood vessels to measure the fluorescence intensity. In fact, in the same fluorescence image, the fluorescence intensity around small or large blood vessels had no significant difference. However, the difference was significant when the perivascular AQP4 was partially missing. Our study indicates that the polarization of perivascular AQP4 of PDN rats was significantly changed. Furthermore, the polarization and expression of AQP4 varied between different CNS regions and between different sized vessels [22]. We also noticed that vascular structures appeared to differ among the three groups. The possible reason is the disrupted binding of CD31 due to vascular endothelial dysfunction and atherosclerosis in the PDN group. In this study, CD31 was only used to locate blood vessels and was not involved in measuring the median fluorescence intensity of AQP4 in the perivascular areas. Therefore, the quantification of AQP4 polarization in this study is reliable and believable. Previous studies have shown that the choice of anesthetic significantly impacts the glymphatic function [23]. In this study, the standards of sevoflurane anesthesia, including the concentration of sevoflurane, the concentration of oxygen, and the mode of anesthesia, are uniform. Most importantly, the duration of anesthesia was basically the same in different rats. Therefore, the effect of sevoflurane anesthesia on AQP4 expression can be offset. Certainly, the effect of sevoflurane anesthesia on AQP4 expression in PDN rats requires further research.

Metformin has been used clinically for decades to treat diabetes, and the possible mechanisms by which it attenuates pain are numerous. In the PDN animal model, metformin can attenuate diabetic neuralgia by activating the AMPK signal pathway and reducing the release of inflammatory cytokines [24,25]. The accumulation of inflammatory factors and other metabolic waste may cause central sensitization and impairment of the glymphatic system. In this study, metformin significantly alleviated mechanical pain in PDN rats, possibly related to the restoration of AQP4 polarization in the glymphatic system of the spinal cord of rats.

Conclusion

In this study, a PDN rat model was established using low-dose STZ intraperitoneal injection combined with a high-fat and high-glucose diet. For PDN rats, the clearance rate of the metabolic waste in the glymphatic system decreased, the AQP4 polarization was reversed, and the protein expression of AQP4 increased. Metformin significantly alleviated mechanical pain in PDN rats. The analgesic effect of metformin on PDN may be associated with restoring the function of the glymphatic system.

Acknowledgements

We sincerely thank Yu Yan, Jingxuan Du, Jingjing Jiang, Jiashuai lv, and Xinxue Xiao (five undergraduates of North Sichuan Medical College) for their assistance in lab work and animal care. We are also grateful to the Hepatobiliary Institute and anesthesia Laboratory of North Sichuan Medical College for providing us with the experimental platform.

This study was supported by the School-level Key Scientific Research Project of North Sichuan Medical College (CBY22-ZDA09), North Sichuan Medical College School-level Scientific Research Youth Project (CBY22-QNA09), and Nanchong Science and Technology Bureau Municipal School Cooperation Project (22SXQT0125).

C. Xu designed the study, prepared the animal ethics and funding applications, conducted the study, and participated in manuscript preparation and revision. F. Wang, S. Can, X. Guo and J. Li participated in animal research. J. Lin conducted the study. All the authors reviewed

and accepted the final manuscript. All authors read and approved the final manuscript.

Availability of data and materials: The datasets are available from the corresponding author on reasonable request.

Ethics approval and consent to participate: all experimental procedures were approved by the ethical committee of North Sichuan Medical College (No.202183).

Video abstract

In order to let readers quickly understand our research report, we made a video abstract, Supplemental Digital Content 1, *http://links.lww.com/WNR/A688*, which briefly introduced the research background, research methods, research results, innovations and future prospects of the experiment.

Conflicts of interest

There are no conflicts of interest.

References

1 Iqbal Z, Azmi S, Yadav R, Ferdousi M, Kumar M, Cuthbertson DJ, *et al*. Diabetic peripheral neuropathy: epidemiology, diagnosis, and pharmacotherapy. *Clin Ther* 2018; **40**:828–849.

2 Zhu D, Fan T, Huo X, Cui J, Cheung CW, Xia Z. Progressive increase of inflammatory CXCR4 and TNF-alpha in the dorsal root ganglia and spinal cord maintains peripheral and central sensitization to diabetic neuropathic pain in rats. *Mediators Inflamm* 2019; **2019**:4856156.

3 Lin JY, Huang XL, Chen J, Yang ZW, Lin J, Huang S, *et al*. Stereological study on the number of synapses in the rat spinal dorsal horn with painful diabetic neuropathy induced by streptozotocin. *Neuroreport* 2017; **28**:319–324.

4 Iliff JJ, Wang M, Liao Y, Plogg BA, Peng W, Gundersen GA, *et al*. A paravascular pathway facilitates CSF flow through the brain parenchyma and the clearance of interstitial solutes, including amyloid β. *Sci Transl Med* 2012; **4**:147ra111.

5 Peng W, Achariyar TM, Li B, Liao Y, Mestre H, Hitomi E, *et al*. Suppression of glymphatic fluid transport in a mouse model of Alzheimer's disease. *Neurobiol Dis* 2016; **93**:215–225.

6 Jiang Q, Zhang L, Ding G, Davoodi-Bojd E, Li Q, Li L, *et al*. Impairment of the glymphatic system after diabetes. *J Cereb Blood Flow Metab* 2017; **37**:1326–1337.

7 Iliff JJ, Lee H, Yu M, Feng T, Logan J, Nedergaard M, *et al*. Brain-wide pathway for waste clearance captured by contrast-enhanced MRI. *J Clin Invest* 2013; **123**:1299–1309.

8 Liu S, Lam MA, Sial A, Hemley SJ, Bilston LE, Stoodley MA. Fluid outflow in the rat spinal cord: the role of perivascular and paravascular pathways. *Fluids Barriers CNS* 2018; **15**:13.

9 Wei F, Zhang C, Xue R, Shan L, Gong S, Wang G, *et al*. The pathway of subarachnoid CSF moving into the spinal parenchyma and the role of astrocytic aquaporin-4 in this process. *Life Sci* 2017; **182**:29–40.

10 Ward R, Li W, Abdul Y, Jackson L, Dong G, Jamil S, *et al*. NLRP3 inflammasome inhibition with MCC950 improves diabetes-mediated cognitive impairment and vasoneuronal remodeling after ischemia. *Pharmacol Res* 2019; **142**:237–250.

11 Harrison IF, Ismail O, Machhada A, Colgan N, Ohene Y, Nahavandi P, *et al*. Impaired glymphatic function and clearance of tau in an Alzheimer's disease model. *Brain* 2020; **143**:2576–2593.

12 Baeza-Flores GDC, Guzmán-Priego CG, Parra-Flores LI, Murbartián J, Torres-López JE, Granados-Soto V. Metformin: a prospective alternative for the treatment of chronic pain. *Front Pharmacol* 2020; **11**:558474.

13 Lin JY, He YN, Zhu N, Peng B. Metformin attenuates increase of synaptic number in the rat spinal dorsal horn with painful diabetic neuropathy induced by type 2 diabetes: a stereological study. *Neurochem Res* 2018; **43**:2232–2239.

14 Iliff JJ, Wang M, Zeppenfeld DM, Venkataraman A, Plog BA, Liao Y, *et al*. Cerebral arterial pulsation drives paravascular CSF-interstitial fluid exchange in the murine brain. *J Neurosci* 2013; **33**:18190–18199.

15 Li L, Chopp M, Ding G, Davoodi-Bojd E, Zhang L, Li Q, *et al*. MRI detection of impairment of glymphatic function in rat after mild traumatic brain injury. *Brain Res* 2020; **1747**:147062.

16 Kress BT, Iliff JJ, Xia M, Wang M, Wei HS, Zeppenfeld D, *et al*. Impairment of paravascular clearance pathways in the aging brain. *Ann Neurol* 2014; **76**:845–861.

17 Plog BA, Nedergaard M. The glymphatic system in central nervous system health and disease: past, present, and future. *Annu Rev Pathol* 2018; **13**:379–394.

18 Mader S, Brimberg L. Aquaporin-4 water channel in the brain and its implication for health and disease. *Cells* 2019; **8**:90.

19 Kitchen P, Salman MM, Halsey AM, Clarke-Bland C, MacDonald JA, Ishida H, *et al*. Targeting Aquaporin-4 subcellular localization to treat central nervous system edema. *Cell* 2020; **181**:784–799.e19.

20 Yan X, Liu J, Wang X, Li W, Chen J, Sun H. Pretreatment with AQP4 and NKCC1 inhibitors concurrently attenuated spinal cord edema and tissue damage after spinal cord injury in rats. *Front Physiol* 2018; **9**:6.

21 Salman MM, Kitchen P, Woodroofe MN, Brown JE, Bill RM, Conner AC, *et al*. Hypothermia increases aquaporin 4 (AQP4) plasma membrane abundance in human primary cortical astrocytes via a calcium/transient receptor potential vanilloid 4 (TRPV4)- and calmodulin-mediated mechanism. *Eur J Neurosci* 2017; **46**:2542–2547.

22 Gundersen GA, Vindedal GF, Skare O, Nagelhus EA. Evidence that pericytes regulate aquaporin-4 polarization in mouse cortical astrocytes. *Brain Struct Funct* 2014; **219**:2181–2186.

23 Hablitz LM, Vinitsky HS, Sun Q, Stæger FF, Sigurdsson B, Mortensen KN, *et al*. Increased glymphatic influx is correlated with high EEG delta power and low heart rate in mice under anesthesia. *Sci Adv* 2019; **5**:eaav5447.

24 Hasanvand A, Amini-Khoei H, Hadian MR, Abdollahi A, Tavangar SM, Dehpour AR, *et al*. Anti-inflammatory effect of AMPK signaling pathway in rat model of diabetic neuropathy. *Inflammopharmacology* 2016; **24**:207–219.

25 Ma J, Yu H, Liu J, Chen Y, Wang Q, Xiang L. Metformin attenuates hyperalgesia and allodynia in rats with painful diabetic neuropathy induced by streptozotocin. *Eur J Pharmacol* 2015; **764**:599–606.